Kinetics and Mechanism of the Sonolytic Degradation of Chlorinated Hydrocarbons: Frequency Effects

Hui-Ming Hung and Michael R. Hoffmann*

W. M. Keck Laboratories, California Institute of Technology, Pasadena, California 91125

Received: December 1, 1998; In Final Form: February 4, 1999

The kinetics of the sonolytic degradation of aqueous solutions of carbon tetrachloride and hexachloroethane (C_2Cl_6) were investigated at six different frequencies over the range from 20 to 1078 kHz. The rates of degradation of CCl_4 and C_2Cl_6 were shown to increase with increasing frequency with optimal degradation rates at 500 kHz. At 205 kHz, the relative rates of sonolytic degradation of the three chlorinated methanes followed the order of $CCl_4 > CHCl_3 > CH_2Cl_2$. Hexachloroethane, which was formed as the primary intermediate in the degradation of CCl_4, was degraded at a rate comparable to that of CCl_4 at all six frequencies.

Introduction

Ultrasound has been used for a wide variety of biological, physical, and chemical applications.[1−6] For example, chlorinated hydrocarbons, which are often used as industrial degreasing agents, are readily degraded to inorganic products during aqueous-phase ultrasonic irradiation.[3,6−9]

The chemical consequences of the ultrasonic irradiation of liquids are due to the phenomenon of acoustic cavitation.[10] In most liquids, cavitation is initiated by excitation of preexisting microbubbles or other inhomogeneities in the fluid such as suspended particles or gas bubble nuclei. The theoretical maximum temperature (T_{max}) and pressure (P_{max}) obtained inside a collapsed cavitation bubble can be calculated from eqs 1 and 2, if the bubble collapse is assumed to be an adiabatic process.[11]

$$T_{max} = T_0\left\{\frac{P_m(\kappa - 1)}{P}\right\} \quad (1)$$

$$P_{max} = P\left\{\frac{P_m(\kappa - 1)}{P}\right\}^{\kappa/(\kappa - 1)} \quad (2)$$

Temperatures near 5000 K have been observed experimentally, while pressures on the order of 1000 bar have been calculated.[12] From the measurement of sonoluminescence during the cavitational collapse of single, isolated bubbles, extreme temperatures (e.g., $>10^3$ K) and pressures (e.g., $>10^3$ atmospheres) have been reported.[13−15]

Dissolved organic compounds are chemically degraded during the sonolysis of aqueous solutions as a direct consequence of the extreme transient conditions of elevated temperature and pressure obtained during cavitational bubble collapse. The three main chemical pathways for compound degradation include (1) hydroxyl radical oxidation, (2) direct pyrolytic degradation, and (3) supercritical water reactions.[16−18] In aqueous solution, water vapor present in the bubble is homolytically split during bubble collapse to yield H$^\bullet$ and $^\bullet$OH radicals, while chemical substrates present either within or near the gas−liquid interface of the collapsing bubble are subject to direct attack by $^\bullet$OH.[16,17] Volatile compounds such as H_2S and CCl_4 readily partition into the vapor of the growing cavitation bubbles and then undergo direct pyrolysis during transient collapse.[3,17,19] In addition, hydrolysis reactions have been observed to be accelerated by several orders of magnitude in the presence of ultrasound. For example, the acceleration in the observed rate of the hydrolysis of *p*-nitrophenyl acetate has been attributed to the existence of transient supercritical water during ultrasonic irradiation.[20]

Carbon tetrachloride (CCl_4), which is one of the most widespread chemical contaminants in the subsurface aquatic environment, is difficult to treat with conventional technologies.[21−30] However, the sonolytic degradation of CCl_4 in water has been shown of to be an effective means for its elimination from contaminated water.[3,7−9] In this regard, Hua and Hoffmann[3] have proposed the following mechanism for the sonolytic degradation of CCl_4 in water ()))) = sonolysis):

$$CCl_4 \xrightarrow{)))} Cl^\bullet + {}^\bullet CCl_3 \quad (3)$$

$$CCl_4 \xrightarrow{)))} Cl_2 + :CCl_2 \quad (4)$$

$${}^\bullet CCl_3 \rightarrow {}^\bullet Cl + :CCl_2 \quad (5)$$

$${}^\bullet CCl_3 + {}^\bullet CCl_3 \rightarrow CCl_4 + :CCl_2 \quad (6)$$

$${}^\bullet CCl_3 + {}^\bullet CCl_3 \rightarrow C_2Cl_6 \quad (7)$$

Dichlorocarbene formed in eq 5 self-reacts to form tetrachloroethylene

$$:CCl_2 + :CCl_2 \rightarrow C_2Cl_4 \quad (8)$$

or it reacts with water to form carbon monoxide and hydrochloric acid

$$:CCl_2 + H_2O \rightarrow 2\,HCl + CO \quad (9)$$

C_2Cl_6 and C_2Cl_4, which are produced as intermediates during the sonolytic degradation of CCl_4, are also readily degraded during aqueous-phase sonication. Chlorine atoms produced in eq 3 rapidly self-react to form molecular chlorine, which hydrolyzes readily to yield hypochlorous, HOCl, and hydrochloric acids

$$2Cl^\bullet \rightarrow Cl_2 \xrightarrow{+H_2O} HOCl + HCl \quad (10)$$

* To whom correspondence should be addressed. Phone: (626) 395-4391. Fax: (626) 395-3170. E-mail: mrh@cco.caltech.edu.

10.1021/jp9845930 CCC: $18.00
Published on Web 03/19/1999

TABLE 1: Physical Dimensions of the Different Frequency Transducers

frequency (kHz)	emitting diameter (cm)	emitting area (cm^2)	sonication volume (mL)
20	1.27	1.27	95
500	5.70	25.5	483
205, 358, 618, 1078	5.48	23.6	605

In this paper, we present the experimental results of a detailed investigation of the sonolytic degradations of $CHCl_3$, CH_2Cl_2, and CCl_4 in aqueous solutions as a function of ultrasonic frequency.

Experimental Procedures

The chlorinated hydrocarbons ($CHCl_3$, CH_2Cl_2, CCl_4) were obtained in high purity and used without further purification. The reagents were obtained from several sources: carbon tetrachloride, CCl_4, 99.9% (J. T. Baker); chloroform, $CHCl_3$, LC grade; dichloromethane, CH_2Cl_2, HPLC grade (EM Science); hexachloroethane, C_2Cl_6, 98% (Aldrich); tetrachloroethene, C_2Cl_4, 99.9% (Sigma-Aldrich). Pentane (Omnisolv grade, EM Science) was used as the analytical solvent for extraction and GC analysis. Aqueous solutions were prepared with purified water obtained from a Milli-Q UV Plus system (18.2 mΩ cm resistivity).

Sonications at frequencies of 205, 358, 618, and 1078 kHz were performed in a glass reactor using an Allied ELAC Nautik ultrasound generator. At 20 kHz ultrasound was generated with a Branson 200 sonifier, and at 500 kHz with an Undatim power generator and transducer. Temperature was maintained constant at 10 °C with a Haake A80 refrigerated bath and circulator. The initial solution temperature is about 13 ± 3 °C. Replaceable titanium tips on the 20 kHz transducers were polished, and the transducer was tuned before each experiment in order to give a minimum power output when vibrating in air. The tuning process is a standard procedure to bring the transducer into resonance as part of the complete probe assembly.[31] Ultrasonic irradiations at 205, 358, 618, and 1078 kHz were carried out in a 605 mL reactor cell, while those at 20 kHz were performed in a 95 mL reactor and those 500 kHz were carried out in a 483 mL reactor. The physical dimensions and characteristics of each transducer and the corresponding reactor configurations are summarized in Table 1 and shown schematically in Figure 1.

Sample aliquots were withdrawn from each respective reactor with a 1 mL Hamilton syringe and filtered through a 0.45 μm nylon filter into a 2.5 mL glass vial containing 0.5 mL of pentane. The glass vials were sealed with a PTFE/silicone septum-lined threaded cap. A 0.5 μL sample of the pentane extract was injected into a HP 5880A gas chromatograph equipped with an electron capture detector (GC-ECD) and operated in the splitless mode using a HP-5 column for the analysis of CCl_4, $CHCl_3$, $H_2C_2Cl_2$, C_2Cl_4, and C_2Cl_6. The GC-ECD was calibrated with chromatographic standards. Duplicate measurements were made for each sample. All sample aliquots were analyzed immediately after collection. The residual aqueous phase in the extraction vials was analyzed by ion-exchange chromatography (IC) for Cl^- using a Dionex Bio-LC system equipped with a conductivity detector and a Dionex OmniPac AS-11 column.

The ultrasonic power output was measured using standard calorimetric procedures.[31] The measured power densities given in Table 2 were used to normalize the observed reaction rate constants (vide infra).

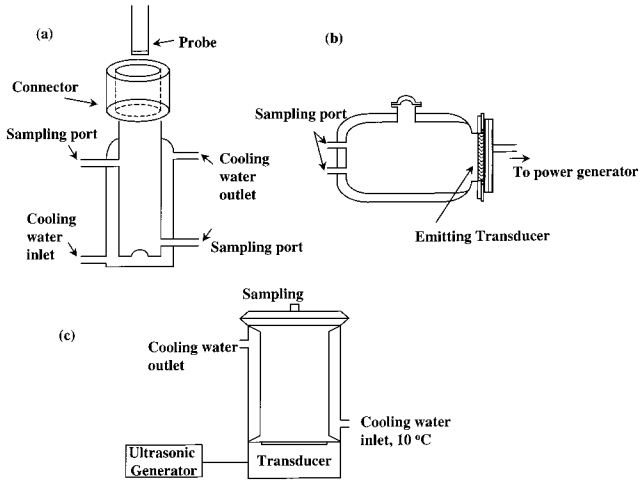

Figure 1. Schematic representation of the reactor cells used in this study: (a) for 20 kHz, (b) for 500 kHz, and (c) for 205, 358, 618, and 1078 kHz.

TABLE 2: Results of Calorimetry Measurements

frequency (kHz)	power output (W)	power density (W/cm^3)
20	62	0.65
500	48	0.10
205, 358, 618, 1078	35	0.06

TABLE 3: Normalized Rate Constants for the Sonolytic Degradation of CCl_4 in Water at $pH_o = 7$, $pH_\infty = 3.5$, and $T = 286$ K with $[CCl_4] = 0.2$ mM

frequency (kHz)	205	358	618	1078	20	500
k $[CCl_4]$ (min^{-1})	0.044	0.049	0.055	0.039	0.025	0.070

Results and Discussion

Frequency Effects. Experiments were performed with initial H_xCCl_{4-x} concentrations set at 0.20 ± 0.05 mM. Under these conditions, the extent of degradation of CCl_4 was found to be greater than 99% after 90 min of sonolysis. Loss of CCl_4 due to vapor stripping was found to be less than 2% in separately run control experiments in the absence of ultrasonic irradiation. pH values after complete sonolytic degradation of CCl_4 were near 3.5, while the principle products were found to be OCl^-, Cl^-, C_2Cl_4, and C_2Cl_6. The final concentrations of HOCl were in the micromolar range at all frequencies.

The sonication of CCl_4 followed simple pseudo-first-order reaction kinetics, in which the slopes of standard linear regressions of the observed $\ln [CCl_4]_t/[CCl_4]_o$ vs time data corresponded to the observed first-order rate constants. To determine the effects of frequency on the observed reaction rates, the observed first-order rate constants at different frequencies were normalized for differences in acoustic energy densities as follows:[32]

$$k_{\mathrm{corr},f} = k_{\mathrm{obs},f}\left(\frac{P_{f_s}}{P_f}\right) \tag{11}$$

where $k_{\mathrm{corr},f}$ and $k_{\mathrm{obs},f}$ are the corrected and the observed rate constants at a given irradiation frequency, f. P_f is the power density, in watts per unit volume at that frequency, and P_{f_s} is the power density at the reference-state ultrasonic frequency, f_s (i.e., 205 kHz). Using the measured power densities as given in Table 2, the rate constants for CCl_4 degradation were corrected relative to the reference standard. These values are listed in Table 3.

As shown in Figure 2, the rate of CCl_4 degradation appears to increase from 205 to 618 kHz and then decreases slightly at

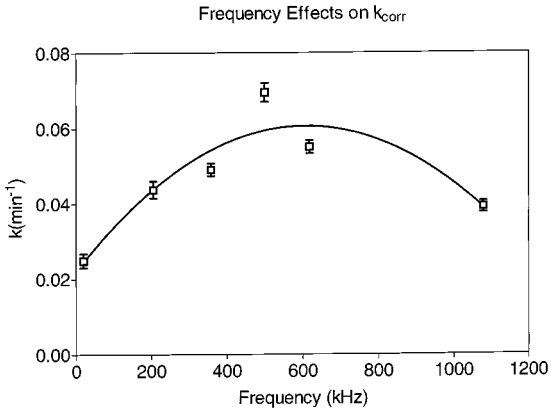

Figure 2. Variation of the CCl_4 degradation rate constant with ultrasonic frequency. Data points are the mean values obtained from multiple experiments.

1078 kHz for the same reactor system. Furthermore, the measured reaction rate in the 500 kHz reactor was found to be substantially larger than that in the 20 kHz reactor. These trends are comparable with those reported previously by Francony et al.[9] (i.e., an increase in observed degradation rate with an increase in ultrasonic frequency). Since the geometry of the reactor and the corresponding transducer may affect the observed reaction rate, the following discussion will focus only on the data obtained for the same reactor and transducer configuration as a function of frequency, where $f = 205$, 358, 618, or 1078 kHz.

The higher degradation rate observed at 618 kHz may be the result of differences in the relative lifetimes and the surface area to volume ratios of the cavitation bubbles at this frequency relative to the other frequencies. At 618 kHz, a stable cavitation bubble will oscillate more frequently per unit time and, thus, will result in more extensive mass transfer of volatile solute (e.g., CCl_4) between the vapor phase of the bubble and the bulk liquid solution. As a result, the CCl_4 degradation rate should be enhanced due to a greater number of bubble events per unit time and due to a more efficient mass transfer of reactive solute from the liquid phase to the vapor phase. Once gas transfer has taken place, CCl_4 is subjected to pyrolytic reactions within the vapor phase of the collapsing bubbles or within the hot interfacial region of bubbles. As shown in eq 12, the resonant radius of an acoustically cavitating bubble is inversely correlated with the ultrasonic frequency.[11,32]

$$R_r^2 = \frac{3\kappa P_0}{\rho \omega_r^2} \tag{12}$$

where ρ is the density of the solution, ω_r is the resonant frequency, R_r is the resonant radius, P_0 is the hydrostatic pressure, and κ ($\kappa = C_p/C_v$) is the polytropic index. The relative differences in the surface area to volume ratios as a function of ultrasonic frequency are illustrated in Table 4. As a consequence, the higher frequencies produce smaller cavitation bubbles with higher surface area to volume ratios. Therefore, the net diffusion of semivolatile reactants between the bubble and the liquid is enhanced.[32] At higher frequencies, more CCl_4 vapor diffuses into the vapor phase of the bubble and into the interfacial region, where it is likely to undergo pyrolytic decomposition. In addition, smaller bubbles produced at higher frequencies require fewer acoustic cycles before they reach the requisite resonant size. Given the greater number of acoustic cycles per unit time at higher frequencies, rectified diffusion occurs more rapidly

TABLE 4: Influence of Frequency on the Bubble Resonance Radius and Surface Area to Volume Ratio

frequency (kHz)	resonant radius (μm)	surface area, A (μm^2)	volume, V (nL)	A/V (μm^{-1})
20	179	4.06×10^5	24.3	0.017
205	17.5	3.87×10^4	0.023	0.17
358	10	1.27×10^4	0.0042	0.30
500	7.2	6.50×10^2	0.00156	0.42
618	5.8	4.25×10^2	0.00083	0.52
1078	3.3	1.40×10^2	0.00016	0.90

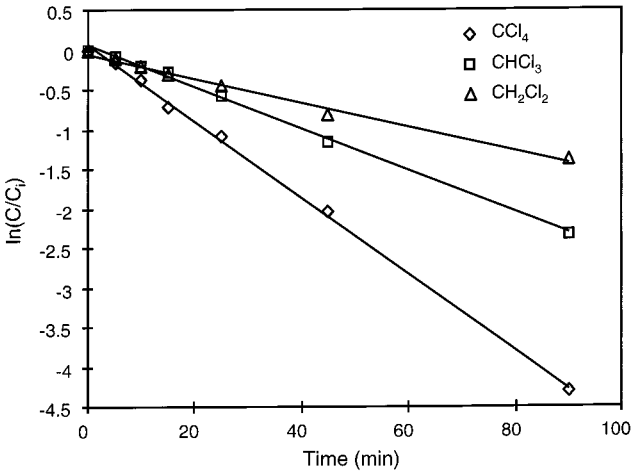

Figure 3. Observed first-order kinetic plots for the degradation of CCl_4, $CHCl_3$, and CH_2Cl_2 at 205 kHz.

TABLE 5: Sonication Rate Constants as a Function of the Henry's Law Constants at 205 kHz with $T = 286 \pm 3$ K

substrate	H (Pa m^3 mol^{-1})	k (min^{-1})
CCl_4	2454	0.044
$CHCl_3$	537	0.028
CH_2Cl_2	200	0.016

before transient bubble collapse. Thus, a greater number of gas nuclei can reach the resonance size more quickly than at lower frequencies. The net effect is to produce a greater enhancement of sonochemical reactions at frequencies up to 700 kHz.[32] However, at 1078 kHz, the cavitation bubbles undergo a stable mode of oscillation for longer times without transient collapse. This results in decreased overall reaction rates as reflected in the data shown in Figure 2 and Table 4.

Sonolysis of Chlorinated Methanes at 205 kHz. The observed rates of sonolytic degradation of CCl_4, $CHCl_3$, and CH_2Cl_2 at 205 kHz at an applied power of 50 W in water are shown in Figure 3. In this series, the rate of CCl_4 degradation was found to be the fastest while CH_2Cl_2 was the slowest. Due to a higher Henry's law constant or larger vapor pressure, more CCl_4 should diffuse into the bubbles and undergo pyrolytic decomposition as the bubbles collapse than will $CHCl_3$ and CH_2Cl_2. For our particular case, $K_H = \gamma_w V_w P^o$ with units of Pa m^3 mol^{-1} where γ_w is the activity coefficient of the chlorinated hydrocarbon in water, V_w is the partial molar volume of water, and P^o is the vapor pressure of the pure organic liquid. A clear relationship between the observed reaction rate constants and the corresponding Henry's law constants is apparent from the data compiled in Table 5.[33] Since the rates of pyrolysis for the chlorinated methanes are rapid, we assume that molecules diffusing into a bubble during a rarefaction cycle will be totally degraded during the corresponding compression cycle. The observed rate constants in this study are given for the following generalized pyrolytic decomposition:

$$CH_xCl_{4-x} \xrightarrow{)))} {}^{\bullet}CH_xCl_{3-x} + {}^{\bullet}Cl \quad (13)$$

while the final observed reaction products for the decomposition of CCl_4, $CHCl_3$, and CH_2Cl_2 were HCl and CO_2. The growth and disappearance of principal intermediates, C_2Cl_4 and C_2Cl_6, obtained during the degradation of CCl_4 and $CHCl_3$ are shown in Figure 4. The primary intermediate observed during $CHCl_3$ sonolysis was C_2Cl_4, while in the case of CCl_4 sonolysis, C_2Cl_6 was found to be the principal intermediate. The difference in the relative behavior of these intermediates, depending on the specific nature of the solute, suggests that somewhat different mechanisms are operative. In the case of $CHCl_3$ sonolysis, the following mechanism is probable:[34]

$$H_2O \xrightarrow{)))} {}^{\bullet}H + {}^{\bullet}OH \quad (14)$$

$$CHCl_3 \xrightarrow{)))} {}^{\bullet}H + {}^{\bullet}CCl_3 \quad (15)$$

$$CHCl_3 \xrightarrow{)))} {}^{\bullet}Cl + {}^{\bullet}CHCl_2 \quad (16)$$

$${}^{\bullet}H + CHCl_3 \rightarrow H_2 + {}^{\bullet}CCl_3 \quad (17)$$

$${}^{\bullet}H + CHCl_3 \rightarrow HCl + {}^{\bullet}CHCl_2 \quad (18)$$

$${}^{\bullet}Cl + CHCl_3 \rightarrow HCl + {}^{\bullet}CCl_3 \quad (19)$$

$${}^{\bullet}OH + CHCl_3 \rightarrow H_2O + {}^{\bullet}CCl_3 \quad (20)$$

In an alternative pathway, the pyrolytic decomposition of $CHCl_3$ may proceed via a molecular elimination reaction to form dichlorocarbene.[35]

$$CHCl_3 \xrightarrow{)))} :CCl_2 + HCl \quad (21)$$

Dichlorocarbenes may then self-react to give C_2Cl_4 as observed by Hua and Hoffmann (3).

$$:CCl_2 + :CCl_2 \rightarrow C_2Cl_4 \quad (22)$$

Since very small concentrations of C_2Cl_6 (i.e., <2 nM) were found during the sonication of $CHCl_3$ compared to that formed during CCl_4 sonication, $CHCl_3$ sonication appears to proceed preferentially via eqs 21 and 22. On the other hand, the sonolytic degradation of CCl_4 has been shown to form the trichloromethyl radical via the direct pyrolysis of a C−Cl bond.[3] After formation, the trichloromethyl radical self-reacts to give C_2Cl_6 or decomposes to form dichlorocarbene according to the reactions of eqs 23−25.

$$CCl_4 \xrightarrow{)))\, k_1} {}^{\bullet}CCl_3 + {}^{\bullet}Cl \quad (23)$$

$$2\,{}^{\bullet}CCl_3 \xrightarrow{k_2} C_2Cl_6 \xrightarrow{)))\, k_3} \text{products} \quad (24)$$

$${}^{\bullet}CCl_3 \xrightarrow{)))\, k_4'} :CCl_2 + {}^{\bullet}Cl \quad (25)$$

$$2{:}CCl_2 \xrightarrow{k_5} C_2Cl_4 \xrightarrow{)))\, k_6} \text{products} \quad (26)$$

If most of ${}^{\bullet}CCl_3$ were decomposed to $:CCl_2$ during CCl_4 sonolysis, then the concentration of C_2Cl_4 should have been higher than C_2Cl_6 as was observed for $CHCl_3$. However, C_2Cl_6 is the principal intermediate observed during CCl_4 sonolysis. In this latter case, the concentration of C_2Cl_6 is approximately 5 times greater than that of C_2Cl_4. This result indicates that the rate of the trichloromethyl radical self-reaction is clearly faster than the rate of ${}^{\bullet}CCl_3$ decomposition. Consistent with this argument is the fact that the rate constant for the self-reaction of the trichloromethyl radicals is to be 10^{10} M^{-1} s^{-1}.[36]

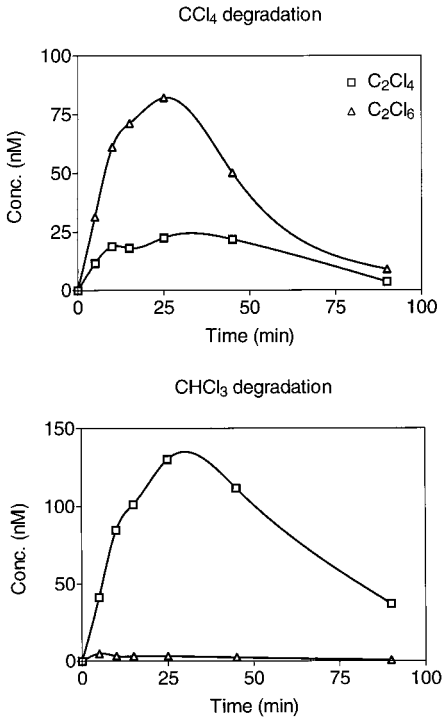

Figure 4. Variations in observed C_2Cl_4 and C_2Cl_6 concentrations vs time during CCl_4 and $CHCl_3$ sonolyses at 205 kHz with an applied power of 50 W and an absorbed power of 35 W.

In a recent study, Kruus et al.[6] reported on their observations of the reaction intermediates produced during the sonication of aqueous chloroform solutions at 900 kHz at an acoustic power of 25 W and an applied power density of 0.17 W cm^{-3}. With an initial concentration of $[CHCl_3]_o = 4.2$ mM, Kruus et al. observed the formation of carbon tetrachloride (18 μM), tetrachloroethene (43 μM), hexachloroethane (32 μM), pentachloroethane (17 μM), trichloroethene (10 μM), 1,1,2,2-tetrachloroethane (3 μM), and hexachlorobutadiene (4 μM) after 10 min of sonication. In contrast, in our system, hexachloroethane and tetrachloroethene were observed as the most substantial reaction intermediates even though chromatographic evidence for the occurrence of CCl_4 and the other intermediates observed by Kruus et al. was obtained. However, the concentrations of these intermediates were barely above the detection limits of the GC-ECD (e.g., ≤1 nM). In addition, we observed the attainment of maximum steady-state concentrations of C_2Cl_6 (1.5 nM) and C_2Cl_4 (130 nM) after 25 min of continuous irradiation of a 0.2 mM chloroform solution at 205 kHz with an applied power of 50 W and an absorbed power density of 0.06 W cm^{-3}. For comparison, Kruus et al.[6] reported that the attainment of the maximum concentrations (vide supra) of all intermediates occurred within the time frame of the first sample aliquot (i.e., collected after 10 min. of irradiation).

Kinetic Analysis. A simple kinetic model can be used to describe the rate of production and subsequent degradation of C_2Cl_6 for the sonolyses of CCl_4. Since the degradation of CCl_4 was observed to be a pseudo-first-order reaction, the reverse reaction of ${}^{\bullet}CCl_3$ and ${}^{\bullet}Cl$ radicals can be ignored. Furthermore,

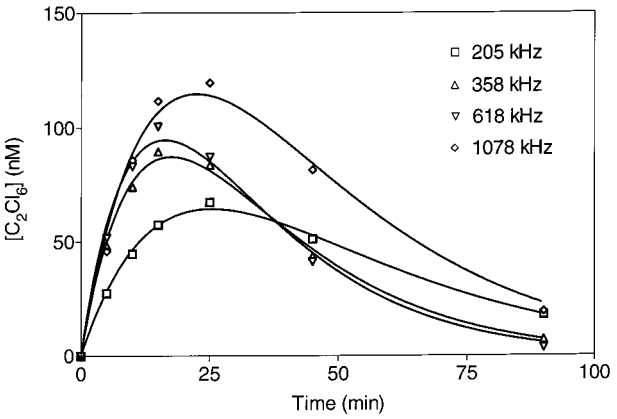

Figure 5. Comparison of experimental and modeled $[C_2Cl_6]$ vs time during CCl_4 sonolysis. Lines are the fitting results from eq 33.

TABLE 6: Reaction Rate Constants Obtained from Kinetic Profiles of $[C_2Cl_6]$ vs Time as a Function of Frequency at 286 ± 3 K

frequency (kHz)	205	358	618	1078	20	500
k_{CCl_4} (min^{-1})	0.044	0.049	0.055	0.039	0.025	0.070
k_1 (min^{-1})	0.045	0.056	0.066	0.045	0.020	0.058
k_3 (min^{-1})	0.042	0.052	0.060	0.042	0.017	0.057

we assume that all of the $^{\bullet}CCl_3$ radicals yield C_2Cl_6. The mechanism of eqs 23 and 24 yields the corresponding kinetic expressions.

$$\frac{d[CCl_4]}{dt} = -k_1[CCl_4] \tag{27}$$

$$\frac{d[^{\bullet}CCl_3]}{dt} = k_1[CCl_4] - 2k_2[^{\bullet}CCl_3]^2 \tag{28}$$

$$\frac{d[C_2Cl_6]}{dt} = k_2[^{\bullet}CCl_3]^2 - k_3[C_2Cl_6] \tag{29}$$

Integration of eq 27 yields

$$[CCl_4] = [CCl_4]_0 e^{-k_1 t} \tag{30}$$

Assuming a steady state for $^{\bullet}CCl_3$,[37]

$$\frac{d[^{\bullet}CCl_3]}{dt} = k_1[CCl_4] - 2k_2[^{\bullet}CCl_3]^2 = 0 \tag{31}$$

we obtain

$$[^{\bullet}CCl_3]_{ss} = \sqrt{\frac{k_1}{2k_2}}[CCl_4]^{1/2} \tag{32}$$

Substitution of $[^{\bullet}CCl_3]_{ss}$ into eq 29 following by integration under the boundary condition of $[C_2Cl_6]_{t=0} = [C_2Cl_6]_{t=\infty} = 0$ yields

$$[C_2Cl_6] = \frac{k_1}{2(k_1 - k_3)}[CCl_4]_0(e^{-k_3 t} - e^{-k_1 t}) \tag{33}$$

The concentration versus time data for the appearance and disappearance of C_2Cl_6 compared to the numerical prediction based on eq 33 is shown in Figure 5. The corresponding observed and normalized rate constants (k_1 and k_3) for C_2Cl_6 as a function of frequency are given in Table 6. As expected, the rate constants, k_1, for all frequencies are very close to those given in Table 3 (which characterizes the total degradation rate of CCl_4). These kinetic results are consistent with a mechanism involving CCl_4 pyrolysis into $^{\bullet}CCl_3$ and $^{\bullet}Cl$ as the rate-limiting step in CCl_4 sonolysis. The degradation rate constant for C_2Cl_6, k_3, is also larger at the higher frequencies and decreases again at 1078 kHz. The calculated degradation rates for C_2Cl_6 in CCl_4 solutions are faster than those in the absence of CCl_4. This may be due to the attack on C_2Cl_6 by the chlorine radicals produced during CCl_4 sonolysis other than $^{\bullet}OH$ only[3] or the assumption of all $^{\bullet}CCl_3$ self-reactions to give C_2Cl_6.

Since the final stable Cl-containing product of CCl_4 sonolysis is Cl^-, we can simplify the overall reaction mechanism in the following way:

$$CCl_4 \xrightarrow{))) k_1} {}^{\bullet}CCl_3 + {}^{\bullet}Cl \tag{34}$$

$$2{}^{\bullet}CCl_3 \xrightarrow{k_2} C_2Cl_6 \tag{35}$$

$$C_2Cl_6 \xrightarrow{))) k_3} aCl^- + \text{other products} \tag{36}$$

$$^{\bullet}Cl + H_2O \xrightarrow{k_4} HCl + {}^{\bullet}OH \tag{37}$$

The mechanisms yields the following kinetic equations:

$$\frac{d[^{\bullet}Cl]}{dt} = k_1[CCl_4] - k_4[^{\bullet}Cl] \tag{38}$$

$$\frac{d[Cl^-]}{dt} = k_4[^{\bullet}Cl] + ak_3[C_2Cl_6] \tag{39}$$

Assuming a steady state for $^{\bullet}Cl$,

$$\frac{d[^{\bullet}Cl]}{dt} = k_1[CCl_4] - k_4[^{\bullet}Cl] = 0 \tag{40}$$

we obtain

$$[^{\bullet}Cl]_{ss} = \frac{k_1}{k_4}[CCl_4] \tag{41}$$

Substitution of $[Cl]_{ss}$ along with eqs 30 and 33 into eq 39 followed by integration under the boundary condition of $[Cl^-]_{t=0} = 0$, yields

$$[Cl^-] = [CCl_4]_0\left[1 - e^{-k_1 t} + \frac{ak_1}{2(k_1 - k_3)}(1 - e^{-k_3 t}) - \frac{ak_3}{2(k_1 - k_3)}(1 - e^{-k_1 t})\right] \tag{42}$$

From the data presented in Table 6, we know that k_1 and k_3 are nearly identical. If we assume $k_3 = k_1 + \delta$ and take the limit of $\delta \rightarrow 0$, we can simplify eq 42 to yield

$$[Cl^-] = [CCl_4]_0\left[\left(1 + \frac{a}{2}\right)(1 - e^{-k_1 t}) - \frac{ak_1 t}{2}e^{-k_1 t}\right] \tag{43}$$

If we further assume that the effect of the second term is small, we can use the following equation as our fitting function for the $[Cl^-]$ vs time data.

$$[Cl^-] = [Cl^-]_\infty(1 - e^{-k_{Cl^-} t}) \tag{44}$$

Based on the curve fitting of our data with eq 44, we obtained

TABLE 7: Values of k_{Cl^-} Obtained from [Cl^-] vs Time Profiles Compared to k_{CCl_4} Values Obtained for the Same Set of Conditions

frequency (kHz)	205	358	618	1078	20	500
k_{CCl_4} (min^{-1})	0.044	0.049	0.055	0.039	0.025	0.070
k_{Cl^-} (min^{-1})	0.042	0.042	0.049	0.031	0.024	0.056

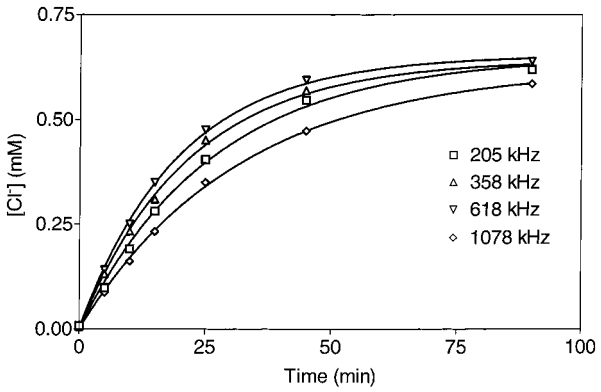

Figure 6. Comparison of experimental and modeled [Cl^-] vs time during CCl_4 sonolysis. Lines are the fitting results from eq 44.

the rate constants, k_{Cl^-}, for Cl^- formation as shown in Table 7 for all frequencies. As expected, k_{Cl^-} is very similar to the rate constant k_1 (Table 7). The experimental and predicted [Cl^-] vs time profiles are shown in Figure 6, while a direct comparison of the specific values for k_{Cl^-} and k_{CCl_4} is given in Table 7.

The total measured Cl^- accounts for only 75% of the total chlorine initially present in the CCl_4. Weissler et al.[2] reported that Cl_2 was produced during the sonolyis of CCl_4 solutions. The total oxidizing chlorine capacity of the released chlorine corresponded closely to four Cl atoms per carbon tetrachloride molecule. However, sonication reactions at higher initial concentrations of carbon tetrachloride, $[CCl_4]_0$, are clearly more complicated. For example, at higher initial concentrations of CCl_4, the initial pyrolysis product, $^{\bullet}CCl_3$ will self-react to give C_2Cl_6, instead of decomposing further via an additional C−Cl bond breaking to produce $:CCl_2$.

In this study, we have demonstrated that the rate of CCl_4 sonolysis increases with increasing frequencies up to 618 kHz and that the principal intermediate product, C_2Cl_6, shows a similar frequency dependence. These results are consistent with general predictions based on underlying physics of acoustic bubble dynamics. At higher frequencies, stable cavitation bubbles oscillate more frequently per second, which leads to enhanced CCl_4 degradation rates. If the cavitation bubbles were to oscillate only in the stable mode without undergoing transient collapse, the net observed reaction rate should be lower as observed at 1078 kHz.

The sonolytic degradation rate constants for the chlorinated methanes were found to increase with a corresponding increase in their respective Henry's law Constants (i.e., $K_{H,CCl_4} > K_{H,CHCl_3} > K_{H,CH_2Cl_2}$) in the order $k_{CCl_4} > k_{CHCl_3} > k_{CH_2Cl_2}$. This relative order is consistent with the argument that the driving force for diffusion into the bubbles is increased as the value of K_H is increased.

Acknowledgment. The authors wish to thank Linda Weavers, Ralf H. Höchemer, Chao-Ping Hsu, and Christian Schiller for their helpful discussions. Financial support from the Office of Naval Research, ONR, and the Department of Energy is gratefully acknowledged.

References and Notes

(1) Mason, T. J.; Lorimer, J. P. *Sonochemistry: Theory, Application and Uses of Ultrasound in Chemistry*; John Wiley & Sons: New York, 1988.

(2) Weissler, A.; Cooper, H. W.; Snyder, S. *J. Am. Chem. Soc.* **1950**, *72*, 1769−1775.

(3) Hua, I.; Hoffmann, M. R. *Environ. Sci. Technol.* **1996**, *30*, 864−71.

(4) Petrier, C.; Micolle, M.; Merlin, G.; Luche, J. L.; Reverdy, G. *Environ. Sci. Technol.* **1992**, *26*, 1639−42.

(5) Cheung, H. M.; Bhatnagar, A.; Jansen, G. *Environ. Sci. Technol.* **1991**, *25*, 1510−12.

(6) Kruus, P.; Beutel, L.; Aranda, R.; Penchuk, J.; Otson, R. *Chemosphere* **1998**, *36*, 1811−1824.

(7) Bhatnagar, A.; Cheung, H. M. *Environ. Sci. Technol.* **1994**, *28*, 1481−6.

(8) Wu, J. M.; Huang, H. S.; Livengood, C. D. *Environ. Prog.* **1992**, *11*, 195−201.

(9) Francony, A.; Petrier, C. *Ultrason. Sonochem.* **1996**, *3*, S77−S82.

(10) Mason, T. J. *Chemistry with Ultrasound*; Elsevisier Applied Science: London, 1990.

(11) Leighton, T. G. *The Acoustic Bubble*; Harcourt Brace & Company: Orlando, 1994.

(12) Shutilov, V. A. *Fundamental Physics of Ultrasound*; Gordon & Breach Science: New York, 1988.

(13) Moss, W. C.; Clarke, D. B.; White, J. W.; Young, D. A. *Phys. Fluids* **1994**, *6*, 2979−2985.

(14) Hiller, R.; Putterman, S. J.; Barber, B. P. *Phys. Rev. Lett.* **1992**, *69*, 1182−1184.

(15) Putterman, S. J. *Scientific Am.* **1995**, *272*, 46−51.

(16) Kotronarou, A.; Mills, G.; Hoffmann, M. R. *J. Phys. Chem.* **1991**, *95*, 3630−8.

(17) Kotronarou, A.; Mills, G.; Hoffmann, M. R. *Environ. Sci. Technol.* **1992**, *26*, 1460−2.

(18) Hua, I.; Hochemer, R. H.; Hoffmann, M. R. *Environ. Sci. Technol.* **1995**, *29*, 2790−6.

(19) Entezari, M. H.; Kruus, P. *Ultrason. Sonochem.* **1994**, *1*, S75−S79.

(20) Hua, I.; Hochemer, R.; Hoffmann, M. R. *J. Phys. Chem.* **1995**, *99*, 2335−2342.

(21) Petrosius, S. C.; Drago, R. S.; Young, V.; Grunewald, G. C. *J. Am. Chem. Soc.* **1993**, *115*, 6131−6137.

(22) Taylor, P. H.; Dellinger, B.; Tirey, D. A. *Int. J. Chem. Kinet.* **1991**, *23*, 1051−1074.

(23) Matheson, L. J.; Tratnyek, P. G. *Environ. Sci. Technol.* **1994**, *28*, 2045−2053.

(24) Johnson, T. L.; Scherer, M. M.; Tratnyek, P. G. *Environ. Sci. Technol.* **1996**, *30*, 2634−2640.

(25) Choi, W. Y.; Hoffmann, M. R. *J. Phys. Chem.* **1996**, *100*, 2161−2169.

(26) Bromberg, L.; Cohn, D. R.; Koch, M.; Patrick, R. M.; Thomas, P. *Phys. Lett. A* **1993**, *173*, 293−299.

(27) Narayanan, B.; Suidan, M. T.; Gelderloos, A. B.; Brenner, R. C. *Water Res.* **1993**, *27*, 181−194.

(28) Loraine, G. A. *Hazard. Waste Hazard. Mater.* **1993**, *10*, 185−194.

(29) Elliott, D. C.; Phelps, M. R.; Sealock, L. J.; Baker, E. G. *Ind. Eng. Chem. Res.* **1994**, *33*, 566−574.

(30) Elliott, D. C.; Sealock, L. J.; Baker, E. G. *Ind. Eng. Chem. Res.* **1994**, *33*, 558−565.

(31) Mason, T. J. *Practical Sonochemistry: User's Guide to Application in Chemistry and Chemical Engineering*; Ellis Horwood: England, 1991.

(32) Hua, I.; Hoffmann, M. R. *Environ. Sci. Technol.* **1997**, *31*, 2237−2243.

(33) Mackay, D.; Shiu, W. Y.; Ma, K. C. *Illustrated Handbook of Physical-Chemical Properties and Environmental Fate for Organic Chemicals*; Lewis: Boca Raton, FL, 1993; Vol. III.

(34) Jennings, B. H.; Townsend, S. N. *J. Phys. Chem.* **1961**, *65*, 1574−1579.

(35) Henglein, A.; Fischer, C. H. *Ber. Bunsen Ges.* **1984**, *88*, 1196−1199.

(36) Matheson, I. A.; Sidebottom, H. W.; Tedder, J. M. *Int. J. Chem. Kinet.* **1974**, *6*, 493−506.

(37) Eyring, H.; Lin, S. H.; Lin, S. M. *Basic Chemical Kinetics*; John Wiley & Sons: New York, 1980.